J. Min. Metall. Sect. B-Metall. 58 (2) (2022) 299 - 310

Journal of Mining and Metallurgy, Section B: Metallurgy

THE EFFECT OF PRECIOUS METALS IN THE NiAl COATING ON THE OXIDATION RESISTANCE OF THE INCONEL 713 SUPERALLOY

M. Zagula-Yavorska*, J. Romanowska

Rzeszow University of Technology, Department of Materials Science, Faculty of Mechanical Engineering and Aeronautics, Rzeszów, Poland

(Received 27 April 2022; Accepted 16 June 2022)

Abstract

The rhodium incorporated aluminide coating was produced by the rhodium electroplating (0.5 μm thick layer) followed by the chemical vapor deposition process on the Inconel 713 superalloy. This coating is composed of the β-NiAl phase. A part of nickel atoms was replaced by rhodium atoms in the β-NiAl phase. The plain, rhodium and platinum incorporated aluminide coatings were oxidized at 1100 ºC under the atmospheric pressure. The oxidation kinetics of the rhodium and platinum incorporated aluminide coatings were similar, but different than oxidation kinetic of the plain coating. The α-Al_2O_3 was the main product both in rhodium and platinum modified coatings after 360 h of oxidation. Moreover, the γ-Ni_3Al phase, besides the β-NiAl phase, was identified. The presence of 4 at. % rhodium in the coating provided similar oxidation resistance as the presence of 10-20 at. % platinum. Both rhodium and platinum incorporated aluminide coatings produced by the chemical vapor deposition process offer good oxidation protection of the Inconel 713 superalloy.

Keywords: *Superalloy; Platinum; Rhodium; Oxidation; Aluminides*

1. Introduction

The inlet gas temperature in the turbine of jet engines can reach about 1650 ºC [1]. Such high temperature and corrosive environment is the reason, why jet engine turbine blades are produced of Ni-based superalloys. However, the Ni-based superalloys are affected by thermal loads and damage due to oxidation [2]. High temperature resistant coatings on Ni-based superalloys are extensively used to prevent oxidation of engine turbine blades [3]. Deposition of thermal barrier coatings on the surface of turbine blades can improve their oxidation resistance [4]. Thermal barrier coatings are composed of metallic bond coatings and ceramic surface coatings. Metallic bond coatings are the Ni(Co)CrAlY type or aluminide ones [5]. Plain aluminides have low density, high thermal conductivity and high melting temperature [6]. An α-Al_2O_3 is formed on the surface of plain aluminide coatings during oxidation. This oxide layer impedes oxygen inward diffusion. However, α-Al_2O_3 that forms on the surface of the plain coating is not continuous. That is why, the oxide layer losses integrity under cyclic oxidation of the plain aluminide coating [7]. Metals of the platinum group (platinum, palladium or iridium) are added to plain aluminide to enhance oxidation resistance of coated superalloys [8-9]. Up to now, platinum is commonly used modifier of aluminide coatings. It is considered that platinum addition improves the oxide layer adherence to the coating [10], inhibits the voids formation under the oxide layer [11], accelerates aluminum diffusivity and favors fast formation of α-Al_2O_3 [12]. Layensa et al. [9] suggest that palladium and iridium act similarly to platinum in the oxidation improvement of aluminide coatings. Despite the beneficial effect of platinum on the oxidation resistance of aluminide coatings, Pint et al. [13] reported that lower rate of oxidation of aluminide coatings was obtained by the zirconium or hafnium incorporation. The minor addition of zirconium (0.04 % at.) to plain aluminide substantially increases oxide adherence to the coating during oxidation [13]. Zirconium segregates at the coating/oxide interface and at the oxide grain boundaries and eliminates stresses in the oxide layer. Yttrium, hafnium, and cerium are also added into the coatings to improve the oxide adherence during oxidation of coated superalloys [14-18]. These elements can be introduced to the superalloy substrates by melting or to the surface of superalloys by the ion implantation or by the MCrAlY overlay coatings deposition [14]. Kim et al. [14] performed yttrium modification of the aluminide coating on the Inconel 713 superalloy. Initially, the Inconel 713

Corresponding author: yavorska@prz.edu.pl

https://doi.org/10.2298/JMMB220427011Z

substrate was pack aluminized, then yttrium layer (1.8 μm thick) was deposited by the ion plating. Hot corrosion test of the yttrium modified aluminide coating and plain aluminide on the superalloy was performed. The aqueous solution of Na_2SO_4 (about 2 mg/cm^2) was sprayed on the coated samples. The sprayed samples were oxidized at 900 °C. It was found that yttrium modification was the effective method to improve corrosion resistance of the coated superalloy. Yttrium localized between α-Al_2O_3 columns, improved the oxide adherence and strongly inhibited aluminum depletion in the aluminide coating. Hafnium reduced the detrimental sulfur effect on the oxide adherences [15]. Hafnium sulfides free energy formation value is negative, so hafnium dissolved in the aluminide coating and as a result, decreases sulfur activity in the superalloy [16]. Liu et al. [17] performed cerium modification of the aluminide coating on the DZ125 superalloy. The modified coatings were deposited by the pack aluminizing process using 1 wt.%, 2 wt.% and 3 wt.% of CeO_2 in the pack mixture. Two-layer structure containing the outer and the diffusion layers was found. The thickness of the diffusion layer decreased when CeO_2 pack mixture content increased. According to Zhang et al. thesis [18], the low content of CeO_2 in the pack led to small diffusion of cerium atoms to the coating. The excess of CeO_2 content in the pack ensured cerium atom packing layer formation on the surface of the sample. The increase of cerium content in the coating from 0.28 to 0.78 wt.% favored the oxidation resistance of the coated superalloy. Cerium reacted with oxygen and CeO_2 formed at the oxide/coating interface. This oxide could prevent internal formation of voids. It is assumed that CeO_2 formed alternative sites for vacancies. Thus vacancy content was limited. The decrease of voids, which resulted from vacancy coalescence, was the reason for the interfacial adhesive strength improvement. The coating with the smallest cerium content (0.28 wt.%) had the most voids, which were distributed at the oxide/coating interface, so it had the poorest oxidation resistance. The coating with the highest cerium content (0.78 wt.%) had the fewest voids, which were distributed at the oxide/coating interface, so the coating had the best oxidation resistance. Despite the good oxidation and hot corrosion resistance, aluminide coatings modified by reactive elements have not been introduced for commercial production.

Chan et al. [19] investigated hot corrosion resistance of the platinum-rhodium modified aluminide coating on the directionally solidified Mar M002 superalloy. Initially, a rhodium layer was electroplated on the superalloy, subsequently a platinum layer was electroplated on the surface of the rhodium coated substrate. The heat treatment of the platinum-rhodium electroplated substrate was performed at 1100 ºC for 1 h in the argon atmosphere. Then the aluminide coating was deposited. The hot corrosion resistance of platinum-rhodium modified aluminide coatings on the superalloy was tested at 900 °C in the sodium sulphate and the sodium chloride environments. The hot corrosion resistance of the platinum-rhodium modified coating was much better than that of only the platinum modified one. Platinum and rhodium acted synergistically in maintaining the β-NiAl phase stability during the hot corrosion test.

Rhodium modification of the aluminide coating was attempted by the Koo et al. [20]. The Inconel 738 superalloy was used as a substrate. A rhodium layer (2-3 μm thick) was electroplated on the superalloy. The pack aluminizing process was used to obtain aluminide coatings on the rhodium electroplated superalloy. The coated specimens were oxidized at 1100 ºC. The aluminide coating with rhodium addition showed slower oxidation rate than plain aluminide and aluminide coatings with palladium addition. The better oxidation resistance of the rhodium modified aluminide coating than the palladium modified one was also found on the CMSX 4 superalloy [21]. The rhodium modified aluminide coatings may be an alternative to palladium modified ones [21].

The crucial issue in improving oxidation resistance of protective coatings is successful implementation of the proper amount of modifiers [8-20]. Oxidation resistance of modified aluminide coatings strongly depends on the correctly carried out electroplating and aluminizing processes. Incorrectness in these processes may result in obtaining coatings with poor oxidation resistance. Unfortunately, until now, there is the lack of data concerning these processes. Therefore, the purpose of this work was to analyze effectiveness of rhodium electroplating followed by chemical vapor deposition processes in obtaining rhodium incorporated aluminide coatings on the Inconel 713 superalloy. The Inconel 713 superalloy was used as a substrate, because it is widely used in the aircraft industry, for instance for turbine blades of aerospace engines. The microstructure of rhodium incorporated aluminide coatings was investigated and the influence of rhodium on the oxidation behavior of the coated Inconel 713 superalloy was determined. There are no literature data whether small rhodium content in the aluminide coating could be as effective as platinum in the oxidation resistance improvement of coated superalloy. Therefore the high temperature oxidation rate of the rhodium incorporated aluminide coating was compared with the plain aluminide coating and platinum incorporated one on the Inconel 713 superalloy.

2. Experimental

A polycrystalline Ni-based Inconel 713 superalloy (chemical composition: 12.0 wt.% Cr, 0.05 wt.% C, 4.6 wt.% Mo, 1.96 wt.% Nb, 5.7 wt.% Al, 0.7 wt.% Ti, 0.19 wt.% Fe, 0.08 wt.% Co, balanced Ni) was the substrate. A rhodium layer (0.5 μm thick) was deposited by the electroplating process on the surface of the Inconel 713 superalloy. The bath for rhodium electroplating was as follows: 0.1 g/dm^3 of rhodium sulfate $Rh_2(SO_4)_3$, 0.15 g/dm^3 of sulfuric acid H_2SO_4, and 0.010g/dm^3 of selenium acid H_2SeO_4. The rhodium electroplated samples were aluminized by the chemical vapor deposition method using the BPXPR0325S equipment manufactured by IonBond Company. Aluminum chloride vapors – $AlCl_3$ were formed in an external generator at 330 °C [22]. The vapors were formed as a result of the flow of the hydrogen chloride - 0.2 l/min via granules of aluminum and then were transported in a hydrogen stream into the chemical vapor deposition reactor where samples of the Inconel 713 were placed. The aluminum chloride vapor reacted with nickel in the samples of the Inconel 713 superalloy and β-NiAl intermetallic phase was formed. Aluminizing in the chemical vapor deposition process consisted of three stages: heating from 20 ºC up to 1040 ºC, aluminizing at 1040 ºC for 600 min, and cooling to the room temperature.

The rhodium incorporated aluminide coating on the Inconel 713 was oxidized at 1100 ºC. The plain and platinum incorporated aluminide coatings were also oxidized [23]. The initial weight of the samples was measured. The oxidation tests were performed at 1100 ºC in the furnace under the atmospheric pressure. The samples were placed in the alumina crucible and then were placed in the furnace heated to 1100 ºC. The samples were kept at 1100 ºC for 20 h and then were cooled down to the room temperature [24]. The weight of the samples after each cycle of oxidation was measured. The samples were cooled down from 1100 ºC to the room temperature in the air.

The cross-sectional microstructural analysis and surface analysis of the unoxidized and oxidized samples were investigated using the scanning electron microscope (SEM) and the energy dispersive spectroscope (EDS). The elemental mapping was analyzed using an electron probe micro-analyzer. The surface phase composition of unoxidized coatings and oxide layers were analyzed by the X-ray diffraction.

3. Results

3.1. Characterization of the aluminized coatings

Fig. 1 showed the cross-sectional microstructure and major elements´ distribution of the rhodium incorporated coating. The coating had an evident two layer microstructure, which included an outer layer and a diffusion layer, below the outer one (Fig. 1a). A large nickel content (about 50 at. %) suggested that coating formation was mainly attributed to nickel outward diffusion (Fig. 1b). The outer and diffusion layers` depth was about 17 and 10 μm, respectively. The highest rhodium content (4 at. %) was in the outer layer, close to the outer/diffusion layers´ interface. The rhodium content decreased towards the coating's surface (only 0.3 at. % rhodium was found at the distance of 5 μm from the surface). The separate light phases in the diffusion layer were analyzed (Fig. 1a). Light phases were enriched with chromium, niobium, and molybdenum (Table 1).

Nickel, aluminium, rhodium, and chromium were found in the outer layer. However, only β-NiAl crystal peaks were visible in XRD patterns (Fig. 2).

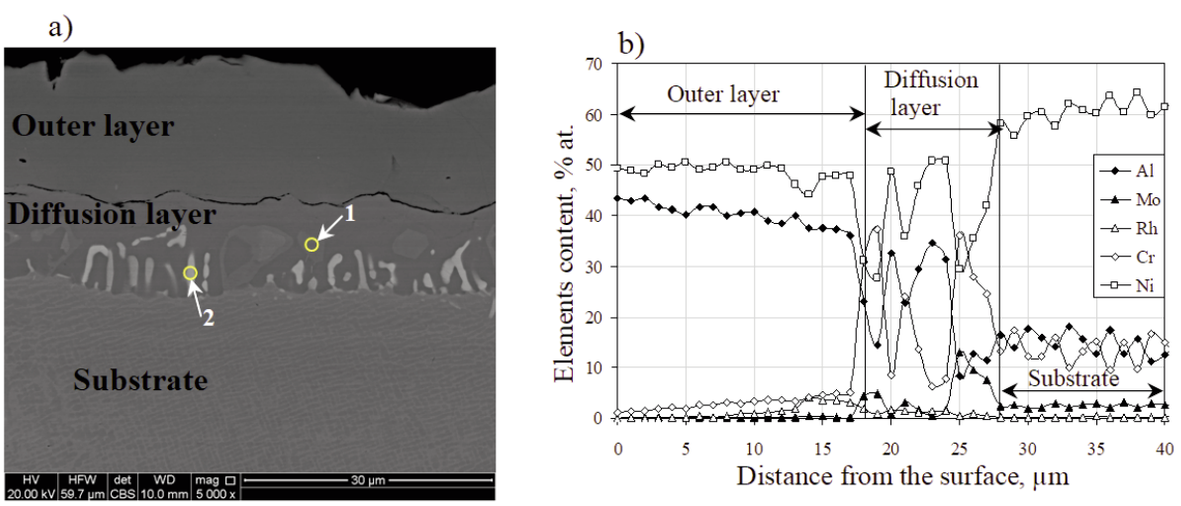

Figure 1. *Cross-sectional microstructure (a) and elements´ distribution (b) of the rhodium incorporated aluminide coating*

Elements such as Cr, Mo, and Nb were localized in the diffusion layer (Fig. 3). Presence of alloying elements (Cr, Mo and Nb) in the diffusion layer was typical for aluminide coatings deposited on superalloys. It proved that alloying elements diffused from the substrate [22-24].

Similar two-layer structure was observed in the platinum modified aluminide coating on the Inconel 713 superalloy. In this case the highest platinum content (10-20 at. %) was in the outer layer of the coating [23].

3.2. *Kinetic curves of coatings' oxidation*

Fig. 4 presented the weight changes of the rhodium incorporated aluminide coating on the Inconel 713 superalloy during oxidation at 1100 ºC. The weight changes of the platinum were incorporated and plain aluminide coating were presented for comparison. The plain aluminide coating showed a rapid weight gain at the first 100 h of oxidation. A weight loss of the plain aluminide occurred after 180 h.

The weight gain of the rhodium incorporated

Table 1. *Cross-sectional chemical composition in spots [at.%], Figure 1a*

Spot	Al	Nb	Mo	Cr	Ni
1	-	-	9.4±0.2	81.5±0.2	9.1±0.3
2	12.2±2.6	8.9±2.0	15.0±4.8	22.6±2.3	41.3±2.0

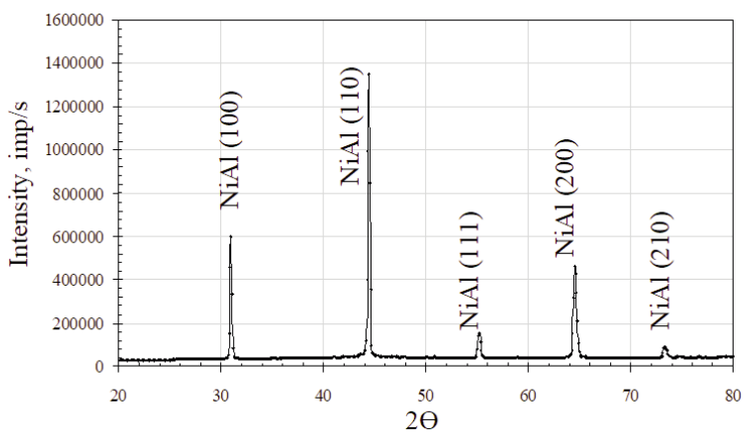

Figure 2. *XRD diffraction of the rhodium incorporated aluminide coating.*

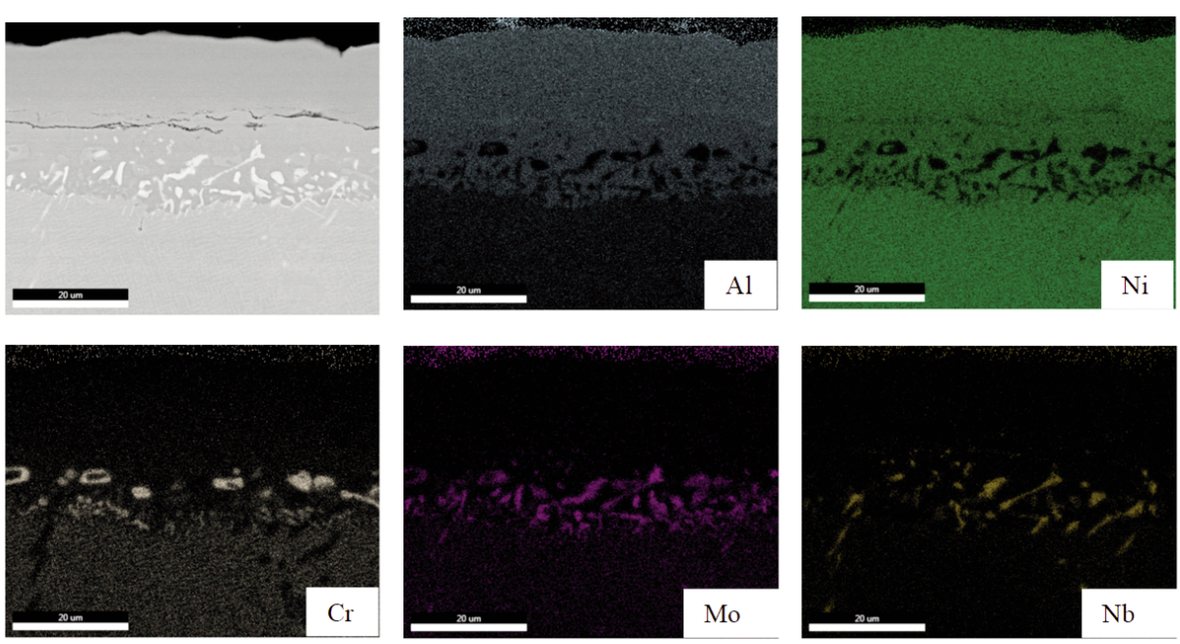

Figure 3. *Elemental mappings of the rhodium incorporated aluminide coating*

coating steadily increased until 400 h of oxidation followed by the weight loss. The oxidation of the rhodium incorporated coating until 700 h did not lead to the loss of its weight. The oxidation resistance of the platinum incorporated coating was similar to that of the rhodium incorporated one. Both rhodium and platinum incorporated aluminide coatings offered reliable oxidation protection of the Inconel 713 superalloy.

3.3. Rhodium or platinum incorporated aluminide coating after oxidation

The surface morphology and surface chemical composition of the oxidized rhodium incorporated coating was presented in Fig. 5 and Table 2. The sample was analyzed after 360 h of cyclic oxidation (18 cycles). The small area of oxide spallation, as well as microckracks of the platinum incorporated aluminide coating were visible after 360 h of cyclic oxidation (18 cycles). For comparison the surface morphology and surface chemical composition analysis of the platinum incorporated aluminide coating after 360 h of oxidation was performed.

The continuous gray oxide layer was formed with a small area of oxide spallation (Fig. 5). The oxide layer consisted of two elements: Al (47.3 at.%) and O (52.7 at.%). The α-Al_2O_3 was detected by the XRD method (Fig. 6). The small peaks for the β-NiAl phase were identified. The quantity of β-NiAl phase, about 0.5 %, was estimated by the Reference Intensity Ration method [25]. Very weak signals from $NiAl_2O_4$, besides intensive signals from α-Al_2O_3, were found (Fig. 6). The cross-sectional microstructure of the rhodium incorporated coating after oxidation with marker of the EDS analysis was presented in Fig. 7, whereas the results of the analysis were shown in Table 3. Predominant elements were: Al (23 at.%) and Ni (71.6 at.%). Moreover, there were Cr (5 at.%) and Rh (0.4 at.%). The chemical composition on the cross-section of coating corresponded to the γ'-Ni_3Al phase (analyzed zone 1 that corresponded to the outer layer of Fig. 1), which was detected by XRD. Except the presence of the γ-Ni_3Al phase, the β-NiAl phase remained (Fig. 6).

It was found that carbides enriched with Cr coarsened, whereas phases enriched with Nb began to dissolve after oxidation (Fig. 8, Table 4).

The surface morphology and surface chemical composition of the platinum incorporated coating was presented in Fig. 9 and Table 5. The continuous gray oxide layer with a small area of oxide spallation, as well as microckracks were formed (Fig. 9). The oxide layer contained 49.5 at.% Al and 50.5 at.% O, no other elements were identified. Very weak signals from $NiAl_2O_4$, besides intensive signals from α-

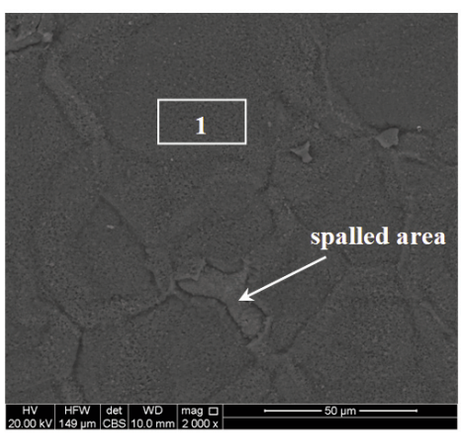

Figure 5. *Surface morphology of the rhodium incorporated aluminide coating after 360 h of oxidation at 1100 °C*

Table 2. *Surface chemical composition in microarea1 [at.%], Figure 5*

Microarea	Al	O
1	47.3±2.1	52.7± 3.9

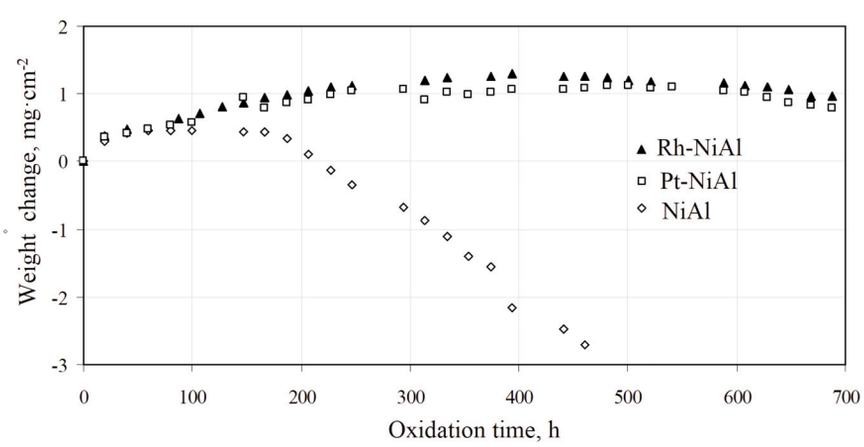

Figure 4. *Weight change curves of the rhodium incorporated (Rh-NiAl), platinum incorporated (Pt-NiAl) and plain aluminide coating (NiAl)*

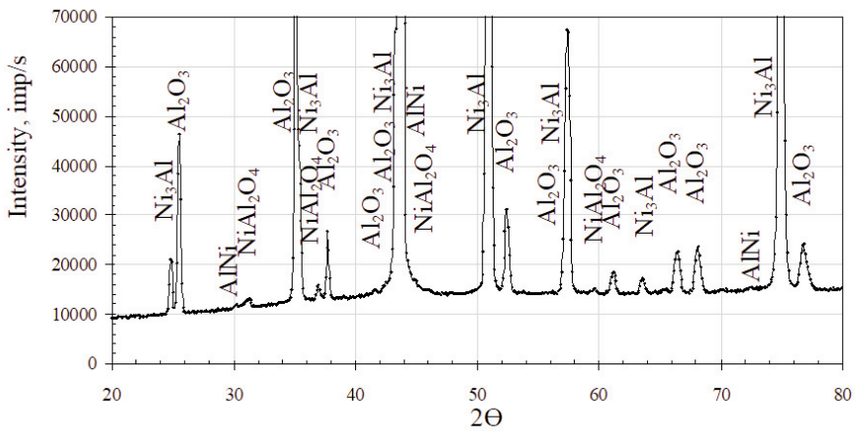

Figure 6. *XRD pattern of the rhodium incorporated aluminide coating after 360 h of oxidation at 1100 ºC*

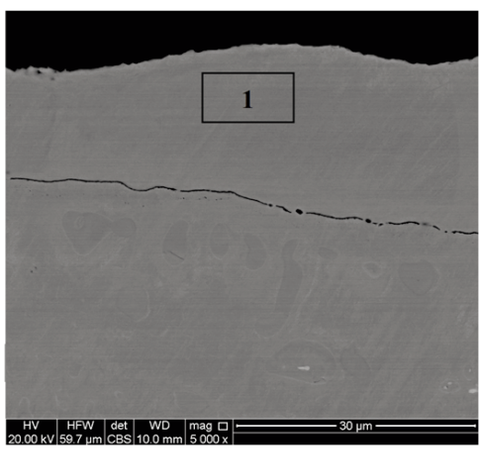

Figure 7. *Cross-sectional microstructure of the rhodium incorporated aluminide coating after 360 h of oxidation at 1100 ºC*

Table 3. *Cross-sectional chemical composition in microarea 1 [at.%], Figure 7*

Microarea	Al	Cr	Ni	Rh
1	23.0±1.9	5±0.2	71.6±1.6	0.4±0.1

Al_2O_3, were found (Fig. 10). This proved that platinum content (10-20 at.%) in the aluminide coating enhanced the α-Al_2O_3 protective layer growth.

The cross-sectional microstructure of the platinum incorporated coating after oxidation with marker of the EDS analysis was presented in Fig.11 and Table 6. Predominant elements were: Al (23.2 at.%) and Ni (70.8 at.%); moreover, there were Cr (3.6 at.%) and Pt (2.4 at.%). Chemical composition on the cross-section of the coating corresponded to the γ-Ni_3Al phase, which was identified by XRD. The β-NiAl phase was also identified by XRD (Fig. 10). The growth of one type of carbides and dissolving of the another type of carbides, similar as in the rhodium incorporated aluminide coating, was noted (Fig. 11).

4. Discussion

Two-layer microstructure of rhodium incorporated aluminide coating was typical for aluminide coatings [26]. Rhodium existed in solid solution in the coating. A part of nickel atoms was replaced by rhodium atoms in the β-NiAl lattice. It can be assumed, that deposition of rhodium was achieved. Refractory elements (Cr, Mo and Nb) were in the diffusion layer (Fig. 3). Carbon present in the superalloy formed carbides with alloying elements (MC type carbide enriched with Ti, Mo, Nb and $M_{23}C_6$ type carbide enriched with Cr and Mo) [27]. Matysiak et al. [28] observed the presence of the primary carbides (MC) enriched with Nb in the cast Inconel 713 superalloy. The stress rupture test that was performed at 980 ºC led to microstructure changes of the superalloy. It was found that at 980 ºC, MC carbides were unstable and decomposed. The most common mechanism of MC carbide decomposition was as follows (1-2) [29]:

$$MC + \gamma \xrightarrow{T,t} M_{23}C_6 + \gamma' \quad (1)$$

$$NbC + (Ni, Mo, Cr, Ti, Al) \rightarrow (Cr, Mo)_{23}C_6 + Ni_3(Al, Ti) + Nb \quad (2)$$

There is strong likelihood that MC-type carbides enriched with Nb and Mo and $M_{23}C_6$-type carbides enriched with Cr and Mo precipitated in the β-NiAl matrix of diffusion layer. MC and $M_{23}C_6$ type carbides were also found in the β-NiAl matrix of diffusion layer of aluminide coatings deposited on the Udimet 700 superalloy [30].

The rapid weight gain of the plain coating at the first 100 h of oxidation may be attributed to the metastable oxide formation at the surface of the coating. The γ- δ- and Θ-Al_2O_3 metastable oxides may be formed in the early period of oxidation. These

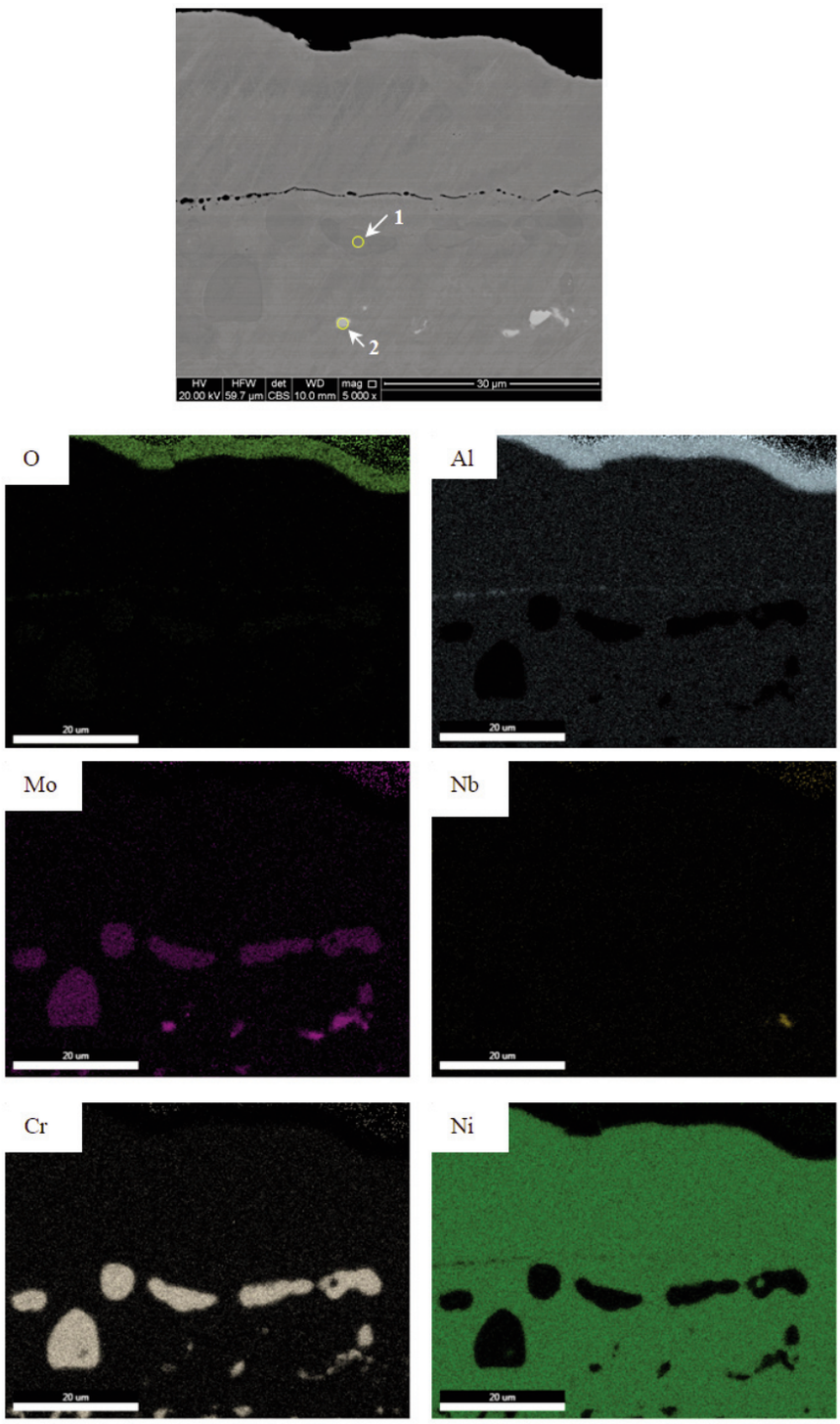

Figure 8. *Elemental mappings of the rhodium incorporated aluminide coating after 360 h of oxidation at 1100 °C*

Table 4. *Cross-sectional chemical composition in spots [at.%], Figure 8*

Spot	Al	Mo	Nb	Cr	Ni
1	1±0.2	9.3±0.3	-	72.4±1.5	17.3±0.7
2	1.8±0.5	48.2±1.9	3.9±2.1	33.8±3.6	12.3±0.2

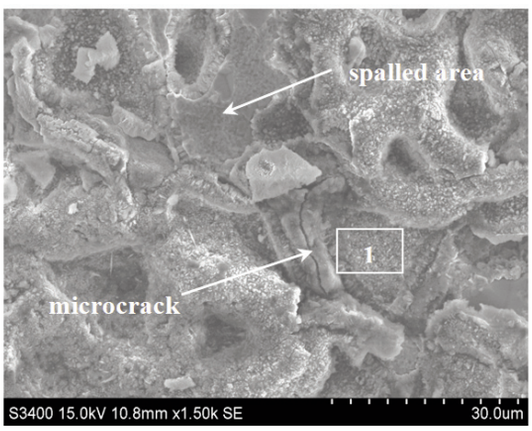

Figure 9. *Surface morphology of the platinum incorporated aluminide coating after 360 h of oxidation at 1100 ºC*

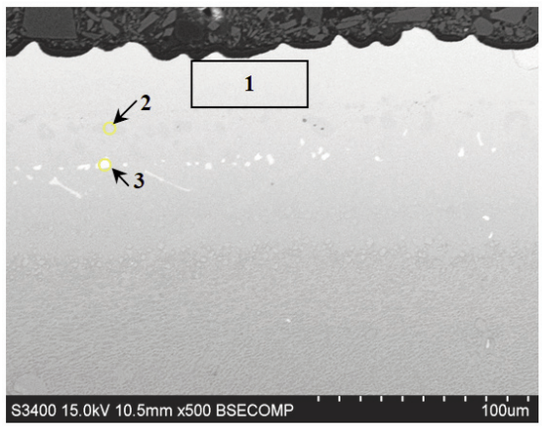

Figure 10. *XRD pattern of the platinum incorporated aluminide coating after 360 h of oxidation at 1100 ºC*

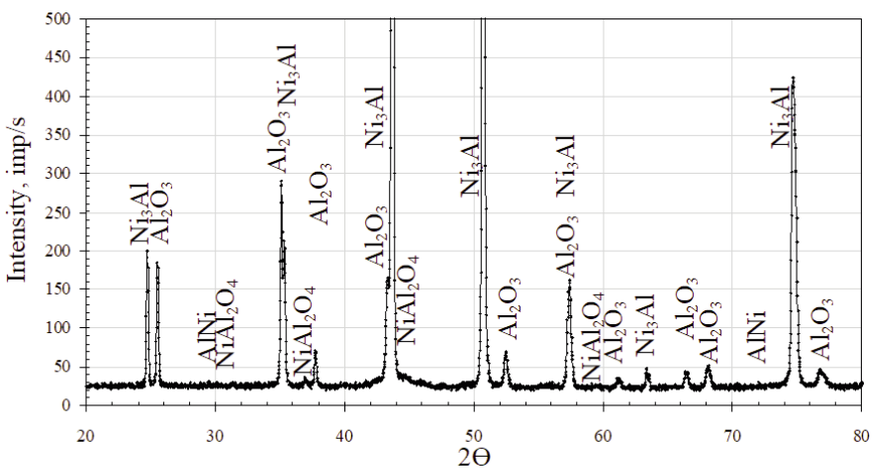

Figure 11. *Cross-sectional microstructure of the platinum incorporated aluminide coating after 360 h of oxidation at 1100 ºC*

Table 5. *Surface chemical composition in microarea 1 [at.%], Figure 9*

Microarea	Al	O
1	49.5±0.5	50.5±1.4

Table 6. Cross-sectional chemical composition in microareas [at.%], Figure 11

Microarea	Al	Cr	Mo	Ni	Pt
1	23.2±1.9	3.6±2.7	-	70.8±1.7	2.4±0.5
2	9.6±1.5	73±1.5	8.5±1.5	8.9±2.4	-
3	7.3±2.1	28.1±2.3	33.8±3.7	30.8±1.5	-

oxides have distinctive morphological features and show a higher growth rate than stable α- Al_2O_3 oxide. Metastable oxides have many vacancies and lattice defects, resulting from rapid outward growth because of aluminum cations outward diffusion. For example, the Θ-Al_2O_3 metastable oxide growth rate is about an order of magnitude higher than the α- Al_2O_3 stable oxide [31]. A weight loss of the plain aluminide coating occurred after 180 h of oxidation. Jiang et al. [32] concluded that the oxidation time at which the weight loss reached a negative value was defined as the lifetime of the coating, so the lifetime of the plain aluminide coating was about 220 h. The oxide layer spallation may be the reason of the rapid weight loss of the plain aluminide.

Small rhodium content (4 at.%) in the aluminide coating enhanced the protective oxide layer formation, as among identified oxides the desirable α-Al_2O_3 was dominant.

The presence of the γ′-Ni_3Al phase was a result of the β-NiAl→γ′- Ni_3Al phase transformation, which occurred due to the depletion of aluminum from the β-NiAl phase during oxidation. According to Swadźba et al. [33] and Haynes et al. [34] the oxides that formed above the γ′-Ni_3Al phase did not consist only of α-Al_2O_3, but contained oxides of other elements, for example Ni. Due to the fact that the γ′-Ni_3Al phase

formed as a result of the depletion of aluminum from the β-NiAl phase, the content of aluminum was too low in this area to keep an oxide that consisted exclusively of α-Al_2O_3, so oxides containing nickel were formed as well. Fan et al. [35] suggested that carbides dissolved gradually when the β-NiAl →γ′-Ni_3Al phase transformation occurred. It may be due to the higher refractory elements solubility in the γ′-Ni_3Al phase than in the β-NiAl phase.

The platinum content in the outer layer was 10-20 at. % [23]. According to the Al-Ni-Pt phase diagram, it was too low to form platinum-rich particles ($AlPt_2$, Al_3Pt_2 or $NiPt_2Al$ phases) [36]. Therefore, platinum dissolved in the β-NiAl phase. It seems that the formation of the platinum incorporated aluminide coating took place in the following way: aluminum reached the surface where platinum was dissolved in nickel and since aluminium had high affinity to nickel the β-(Ni,Pt)Al phase was formed [37]. Lamesle et al. [38] indicated that mechanisms of platinum aluminide coating formation were similar to mechanisms of palladium modified aluminide coating formation. The rhodium content in the coating was 4 at. %. Similarly as for platinum, according to the Al-Ni-Rh phase diagram, it was too low to form rhodium-rich particles (Al_9Rh_2, Al_5Rh_2 or $Al_{76}Ni_4Rh_{20}$ phases) [39]. Therefore, it seems that the formation of the rhodium incorporated aluminide coating was similar to the platinum incorporated one: aluminum reached the surface where rhodium was dissolved in nickel and since aluminium had high affinity to nickel, the β-(Ni,Rh)Al phase was formed.

The experimental results of this work indicate, that rhodium incorporated to the aluminide coating manufactured by the chemical vapor deposition process at 1040 ºC. This coating was composed of the β-NiAl phase in contrast to rhodium incorporated aluminide coating obtained by the pack cementation method [20], where besides the β-NiAl phase the brittle δ-Ni_2Al_3 phase was identified. The combination of the following processes were compared: rhodium electroplating (2-3 μm thick layer) followed by aluminizing by the pack cementation process at 900 ºC which resulted in obtaining (2-3 at. %) rhodium in the aluminide coating [20]; and rhodium electroplating (0.5 μm thick layer) followed by aluminizing by the chemical vapor deposition process at 1040 ºC which resulted in obtaining 4 at. % rhodium in the coating. The rhodium incorporated aluminide coatings obtained by the chemical vapor deposition process or by the pack cementation process efficiently protected superalloys from oxidation. It may be assumed that, rhodium electroplating (0.5 μm thick layer) followed by the chemical vapor deposition process at 1040 ºC led to obtain rhodium incorporated aluminide coatings that provided such good oxidation resistance of superalloys as coatings obtained by the rhodium electroplating (2-3 μm thick layer) followed by the pack cementation process at 900 ºC. Moreover, it is worth mentioning, that in both coatings the rhodium content was similar (2-4 at. %), but in this process only a 0.5 μm thick rhodium layer was deposited, while in the process proposed by Koo et al. [20] 2-3 μm thick rhodium layer was deposited. Both processes provided good oxidation resistance of superalloys, but the process proposed in this work seems to be cheaper due to a thinner rhodium layer. Platinum and rhodium incorporated aluminide coatings showed better oxidation resistance compared to the plain one. The oxidation rate and tendency of oxide layer spallation of plain aluminide was larger than of the modified one [40-41].

The α-Al_2O_3 oxide layer on the plain, rhodium or platinum incorporated aluminide coating was formed in the initial stage of oxidation according to the reaction (3) [2]:

$$4/3Al(s) + O_2(g) = 2/3Al_2O_3(s) \quad (3)$$

The standard Gibbs free energy of Al_2O_3 formation ΔG_{Al2O3} is as follows (4) [2]:

$$\Delta G_{Al_2O_3} = -1127 + 0.22T \quad (4)$$

The standard Gibbs free energy value of the α-Al_2O_3 oxide formation at 1373 K is - 824.94 KJ/mol of oxygen. The negative value of the standard Gibbs free energy indicated that the formation of that oxide was possible.

Aluminum supported the α-Al_2O_3 layer formation and inward substrate diffusion during oxidation. The β-NiAl to γ′-Ni_3Al phase transformation proceeded according to equation 5 [42]:

$$3\beta - NiAl + 3/2O_2 \rightarrow \gamma' - Ni_3Al + Al_2O_3 \quad (5)$$

Oxide spalling of the plain aluminide coatings started after 150 hours of oxidation, whereas oxide scale spalling of platinum or rhodium incorporated aluminide coatings started after 360 h of oxidation and was significantly slower (Fig.4). That is why EDS and XRD analyses were performed after 360 hours of oxidation, when the modified coatings were still protective. They consisted mainly of aluminum (Fig. 5, 9) and Al_2O_3 and γ′-Ni_3Al phases (Fig. 6, 10), whereas the plain coating consisted mainly of nickel (75 at.%) with low content of chromium (5.30 at.%) and aluminum (18.7 at.%) [40].

The γ′-Ni_3Al phase formed as the uniform layer under the oxide layer. Oxide surface moved inward, as a result of the volume shrinkage. As the oxidation time increased, the β-NiAl to γ′- Ni_3Al phase transformation continued and the volume of coating reduced [41]. The difference of the height of grain

cores and boundaries increased and the surface of the coating became rougher [43]. The β-NiAl phase had better oxidation resistance than the γ′- Ni_3Al phase oxidation [41], so the β-NiAl to γ′-Ni_3Al phase transformation increased the coating's instability during oxidation and accelerated rumpling of the surface of the coating [44].

The α-Al_2O_3 was formed by the simultaneous outward diffusion of aluminum and inward diffusion of oxygen at the beginning of oxidation [43]. The diffusion of aluminum and oxygen became stable when oxidation time increased. Then, aluminum oxide mono-layer of equiaxed grains got thicker. Platinum rich particles precipitated at the α-Al_2O_3 grain boundaries. Consequently, the aluminum ions outward diffusion along grain boundaries was delayed. Aluminum cations reacted with oxygen anions at the oxide/coating border. The oxide/coating border moved inwardly and α-Al_2O_3 columnar grains formed beneath the equiaxed α-Al_2O_3 grains. The diffusion of oxygen anions was slower than that of aluminum cations in the Al_2O_3, so the aluminum oxide growth rate was reduced [45]. Platinum rich precipitates in the oxide layer changed the diffusion process from simultaneous aluminum and oxygen diffusion to predominant inward oxygen diffusion and this could slow down the rate of the α-Al_2O_3 growth. The oxidation resistance of the rhodium incorporated coating was similar to the platinum incorporated one. As rhodium is a platinum group element, it is possible that rhodium rich precipitates in the oxide layer could change the diffusion process from simultaneous aluminum and oxygen diffusion to predominant inward oxygen diffusion and this could slow down the rate of the α-Al_2O_3 growth.

5. Conclusions

The rhodium incorporated aluminide coating was produced by the rhodium electroplating on the superalloy followed by the chemical vapor deposition process. The phase analysis revealed that the coating was composed of the β-NiAl phase. The combination of the processes: rhodium electroplating (0.5 μm thick layer) and followed by aluminizing by the chemical vapor deposition at 1040 ºC resulted in obtaining 4 at. % rhodium in the coating at the outer/diffusion layers′ interface. A part of nickel atoms was replaced by rhodium atoms in the β-NiAl phase. The rhodium incorporated aluminide coatings deposition process proposed in this work seemed to be cheaper than that proposed by Koo et al. [20]. The α-Al_2O_3 was the main product both in rhodium and platinum incorporated coatings after 360 h of oxidation. Despite the fact that the γ′-Ni_3Al phase was identified after 360 h of oxidation, both rhodium and platinum incorporated coatings showed good oxidation resistance, much better than plain aluminide coating. Both rhodium and platinum incorporated aluminide coatings offered reliable oxidation protection of the Inconel 713 superalloy.

Acknowledgments

This research was supported by the National Science Centre, Poland (NCN), project number 2016/21/D/ST8/01684. The authors are grateful to Paweł Koprowski for performing SEM analysis.

Author′s contributions

Conceptualization: M. Zagula-Yavorska; Methodology: M. Zagula-Yavorska; Writing —review and editing: M. Zagula-Yavorska and J. Romanowska. Authors read and agreed to the published version of the manuscript.

Declarations

Conflict of interest: The authors declared that they have no conflict of interest to this work.

References

[1] R. Sitek, P. Kwaśniak, M. Sopicka-Lizer, J. Borysiuk, J. Kamiński, J. Mizera, K. Kurzydłowski, Experimental and ab-initio study of the Zr- and Cr-enriched aluminide layer produced on an IN 713C Inconel substrate by CVD; investigations of the layer morphology, structural stability, mechanical properties and corrosion resistance, Intermetallics, 74 (2016) 15-24. https://doi.org/10.1016/j.intermet.2016.04.003

[2] W. Li, J. Sun, S. B. Liu, Y. Liu, L. Fu, T. G. Wang, S. M. Jiang, J. Gong, C. Sun Preparation and cyclic oxidation behaviour of Re doped aluminide coatings on a Ni-based single crystal superalloy, Corrosion Science,164 (2020) 108354. https://doi.org/10.1016/j.corsci.2019.108354

[3] T. Kepa, G. Bonnet, F. Pedraza, Oxidation behaviour of ultrafast slurry aluminized nickel, Surface and Coating Technology, 424 (2021) 127667. https://doi.org/10.1016/j.surfcoat.2021.127667

[4] K. Mondal, L. Nuñez, C. M. Downey, I. J van Rooyen, Recent advances in the thermal barrier coatings for extreme environments, Material Science for Energy Technologies, 4 (2021) 208-210. https://doi.org/10.1016/j.mset.2021.06.006

[5] M. M. Barjesteh, S. M. Abbasi, K. Zangeneh-Madar, K. Shirvani, Creep rupture properties of bare and coated polycrystalline nickel-based superalloy Rene80, Journal of Mining and Metallurgy, Section B: Metallurgy, 57(3) (2021) 401-412. https://doi.org/10.2298/JMMB201203036B

[6] M. M. Barjesteh, K. Zangeneh-Madar, S. M. Abbasi, K. Shirvani, The effect of platinum-aluminide coating features on high temperature fatigue life of nickel-based superalloy Rene80, Journal of Mining and Metallurgy, Section B: Metallurgy, 55(2) (2019) 235-251. https://doi.org/10.2298/JMMB181214029B

[7] S. Nouri, M. Azadeh, Microstructural investigation of the coatings prepared by simultaneous aluminizing and siliconizing process on γ-TiAl, Journal of Mining and Metallurgy, Section B: Metallurgy, 55(2) (2019) 217-225. https://doi.org/10.2298/JMMB180814021N

[8] C. Y. Jiang, L. Y. Qian, M. Feng, H. Liu, Z. B. Bao, M. H. Chen, S. L. Zhu, F. H. Wang, Benefits of Zr addition to oxidation resistance of a single-phase (Ni,Pt) Al coating at 1373 K, Journal of Materials Science and Technology, 35 (2019) 1334–1344. https://doi.org/10.1787/5jxrjncwxv6j-en

[9] C. Leyensa, B. A. Pint, I. G. Wright, Effect of composition on the oxidation and hot corrosion resistance of NiAl doped with precious metals, Surface and Coating Technology, 2 (2000) 15-22. https://doi.org/10.1016/S0257-8972(00)00878-1

[10] S. G. Lakshmi, K. T. Swarup, D. K. Das, M. Roy, Erosion behaviour of platinum aluminide bond coat on directionally solidified CM247 and AM1 single crystal superalloys, Surface and Coating Technology, 429 (2022) 127941. https://doi.org/10.1016/j.surfcoat.2021.127941

[11] P. Y. Hou, V. K. Tolpygo, Examination of the platinum effect on the oxidation behavior of nickel-aluminide coatings, Surface and Coating Technology, 202 (2007) 623–627. https://doi.org/10.1016/j.surfcoat.2007.06.013

[12] M. K. Kumawat, R. Sarkar, V. Jayaram, M. Z. Alam, Fatigue behavior of a freestanding Pt-aluminide (PtAl) bond coat at ambient temperature, Surface and Coating Technology, 427 (2021) 127787. https:// doi.org/10.1016/j.surfcoat.2021.127787

[13] B. A. Pint, I. G. Wright, W. Y. Lee, Y. Zhang, K. Prüßner, K. B. Alexander, Substrate and bond coat compositions: factors affecting alumina scale adhesion, Materials Science and Engineering A, 245 (1998) 201–211. https://doi.org/10.1016/S0921-5093(97)00851-4

[14] K. Kim, J. Jun, J. Lee, High temperature corrosion on yttrium modified aluminide coatings on IN 713 C, Journal de Physique IV, 3 (1993) 521-529. https://doi.org/10.1051/jp4:1993955

[15] L. Yang, M. Chen, J. Wang, Y. Qiao, P. Guo, S. Zhu, F. Wang, Microstructure and composition evolution of a single-crystal superalloy caused by elements interdiffusion with an overlay NiCrAlY coating on oxidation, Journal of Materials Science and Technology, 45 (2020) 49-58. https://doi.org/10.1016/j.jmst.2

[16] S. Li, M. M. Xu, C. Y. Zhang, Y. S. Niu, Z. B. Bao, S. L. Zhu, F. H. Wang, Co-doping effect of Hf and Y on improving cyclic oxidation behavior of (Ni,Pt)Al coating 1150 °C, Corrosion Science, 178 (2021) 109093. https://doi.org/10.1016/j.corsci.2020.109093

[17] Z. Liu, X. Zhao, H. Guo, Ch. Zhou, Cyclic oxidation resistance of Ce/Co modified aluminide coatings on nickel base superalloys, Corrosion Science, 94 (2015) 135–141. https://doi.org/10.1016/j.corsci.2015.01.050

[18] Y. Zhang, X. P. Guo, Effect of CeO_2 on microstructure and oxidation resistance of silicide coatings prepared on Nb-silicide-based ultrahigh temperature alloy, The Chinese Journal of Nonferrous Metals, 23 (2013) 99–107.

[19] W. Y. Chan, P. K. Datta, G. Fisher, J. S. Burnell-Gray, The hot corrosion resistance of platinum–rhodium modified diffusion coating on directionally solidified MAR M002 superalloy at 900°C, High Temperature Surface Engineering, 1-10 (2000). https://doi.org/10.1201/9780367814069

[20] ChH. Koo, ChY. Bai, Yi-Jun Luo, The structure and high temperature corrosion behavior of pack aluminized coatings on superalloy IN-738LC, Materials Chemistry and Physics, 86 (2004) 258–268.https://doi.org/10.1016/j.matchemphys.2004.01.004

[21] M. Zagula-Yavorska, Oxidation behavior of non-modified and rhodium-or palladium-modified aluminide coatings deposited on CMSX-4 superalloy, Metals, 8 (2018) 613-618. https://doi.org/10.3390/met8080613

[22] M. Zagula-Yavorska, M. Wierzbińska, J. Sieniawski, Rhodium and hafnium influence on the microstructure, phase composition and oxidation resistance of aluminide coatings, Metals, 7(12) (2017) 548. https://doi.org/10.3390/met7120548

[23] M. Zagula-Yavorska, J. Sieniawski, T. Gancarczyk, Some properties of platinum and palladium modified aluminide coatings deposited by CVD method on nickel-base superalloys, Archives of Metallurgy and Materials, 57 (2012) 503-509. https://doi.org/10.2478/v10172-012-0052-1

[24] J. Romanowska, J. Morgiel, M. Zagula-Yavorska, The influence of Pd and Zr co-doping on the microstructure and oxidation resistance of aluminide coatings on the CMSX-4 nickel superalloy, Materials, 14(24) (2021) 7579. https://doi.org/10.3390/ma14247579

[25] C. R. Hubbard, E. H. Evans, D. K. Smith, The reference intensity ratio, I/Ic, for computer simulated powder patterns, Journal of Applied Crystallography, 9 (1976) 169-174. https://doi.org/10.1107/S0021889876010807

[26] J. Romanowska, J. Morgiel, M. Zagula-Yavorska, J. Sieniawski, Nanoparticles in hafnium-doped aluminide coatings. Materials Letters, 145 (2015) 162-166. https://doi.org/10.1016/j.matlet.2015.01.089

[27] S. Bose, High Temperature Coatings, Burlington, 2007

[28] H. Matysiak, M. Zagorska, A. Balkowiec, B. Adamczyk-Cieslak, R. Cygan, J. Cwajna, J. Nawrocki, K. Kurzydłowski, The microstructure degradation of the In 713C nickel-based superalloy after the stress rupture tests, Journal of Materials Engineering and Performance, 23 (2014) 3305-3313. https://doi.org/10.1007/s11665-014-1123-4

[29] ASM International, Handbook Committee, Nickel, Cobalt and Their Alloys; J.R. Davis, Ed., ASM International, Almere, 2000

[30] G. W. Goward, D. H. Boone, Mechanisms of formation of diffusion aluminide coatings on nickel-base superalloys, Oxidation of Metals, 3 (1971) 475–495. https://doi.org/10.1007/BF00604047

[31] P. Zhang, Performance of MCrAlX coatings: Oxidation, Hot Corrosion and Interdiffusion, Linköping, 2019

[32] C. Jiang, L. Qian, M. Feng, H. Liu, Z. Bao, M. Chen, S. Zhu, F. Wang, Benefits of Zr addition to oxidation resistance of a single-phase (Ni,Pt)Al coating at 1373 K, Journal of Materials Science and Technology, 35 (2019) 1334–1344. https://doi.org/10.1016/j.jmst.2019.03.013

[33] R. Swadźba, M. Hetmańczyk, J. Wiedermann, L. Swadźba, G. Moskal, B. Witala, K. Radwański, Microstructure degradation of plain, Pt- and Pt+Pd-

modified aluminide coatings on CMSX-4 superalloy under cyclic oxidation conditions, Surface and Coating Technology, 215 (2013) 16-23. https://doi.org/10.1016/j.surfcoat.2012.06.093

[34] J. Haynes, Y. Zhang, W. Lee, B. Pint, I. Wright, K. Cooley, J. Hampikian, Elevated Temperature Coatings: Science and Technology III, TMS, Warrendale, 1999

[35] Q. Fan, H. Yu, T. Wang, Z. Wu, Y. Liu, (2018) Microstructure and oxidation resistance of a Si doped platinum modified aluminide coating deposited on a single crystal superalloy, Coatings, 8 (2018) 1–12. https://doi.org/10.3390/coatings8080264

[36] B. Grushko, D. Kapush, V. Konoval, V. Shemet, A study of the Al-Ni-Pt alloy system. Phase equilibria at 1100 and 1300°C, Powder Metallurgy and Metals Ceramics, 50 (2011) 462-270. https://doi.org/10.1007/s11106-011-9350-9

[37] J. Benoit, K. Badawi, A. Malié, C. Ramade, Microstructure of Pt-modified aluminide coatings on Ni-based superalloys, Surface and Coating Technology, 182(1) (2004) 14-23. https://doi.org/10.1016/S0257-8972(03)00871-5

[38] P. Lamesle, P. Steinmetz, Growth mechanisms and hot corrosion resistance of palladium modified aluminide coatings on superalloys, Materials and Manufacturing Processes, 10 (2009) 1053-1075. https://doi.org/10.1080/10426919508935088

[39] B. Przepiórzyński, S. Mi, B. Grushko, M. Surowiec, An investigation of the Al-Ni-Rh phase diagram between 50 and 100 at% Al, Intermetallics, 15 (2007) 918–928. https://doi.org/10.1016/j.intermet.2006.10.051

[40] M. Zagula-Yavorska, J. Sieniawski, Microstructural study on oxidation resistance of nonmodified and platinum modified aluminide coating, Journal of Materials Engineering and Performance, 23 (2014) 918–926. https://doi.org/10.1007/s11665-013-0841-3

[41] M. Zagula-Yavorska, J. Sieniawski, Cyclic oxidation of palladium modified and nonmodified aluminide coatings deposited on nickel base superalloys, Archives of Metallurgy and Materials, 8 (2018) 130–139. https://doi.org/10.1016/j.acme.2017.05.004

[42] W. Li, L. B. Fu, Y. D. Liu, W. L. Zhang, T. G. Wang, S. M. Jiang, J. Gong, C. Sun, The role of Re in effecting isothermal oxidation behavior of β-(Ni,Pt)Al coating on a Ni-based single crystal superalloy, Corrosion Science, 176 (2020) 108892. https://doi.org/10.1016/j.corsci.2020.108892

[43] Y. Yang, C. Jiang, H. Yao, Z. Bao, S. Zhu, F. Wang, Cyclic oxidation and rumpling behaviour of single phase β-(Ni,Pt)Al coatings with different thickness of initial Pt plating, Corrosion Science, 111 (2016) 162-174. https://doi.org/10.1016/j.corsci.2016.05.011

[44] J. M. Aurrecoechea, L. L. Hsu, K. G. Kubarych, Field experience of platinum aluminide coated turbine blades Materials and Manufacturing Processes, 10 (2009) 1037-1051. https://doi.org/10.1080/10426919508935087

[45] M. S. Li, P. Y. Hou, Improved Cr_2O_3 adhesion by Ce ion implantation in the presence of interfacial sulfur segregation, Acta Materialia, 55 (2007) 443–453. https://doi.org/10.1016/j.actamat.2006.07.047

UTICAJ PLEMENITIH METALA U NiAl PREVLACI NA OTPORNOST NA OKSIDACIJU SUPERLEGURE INCONEL 713

M. Zagula-Yavorska*, J. Romanowska

Tehnološki univerzitet u Žešovu, Odsek za nauku o materijalima, Fakultet za mašinstvo i aeronautiku, Žešov, Poljska

Apstrakt

Aluminidna prevlaka sa rodijumom dobijena je galvanizacijom rodijuma (sloj debljine 0,5 μm), nakon čega je usledio proces hemijske depozicije pare na Inconel 713 superleguri. Ova prevlaka se sastojala od β-NiAl faze. Deo atoma nikla je zamenjen atomima rodijuma u β-NiAl fazi. Obične rodijumske i platinaste aluminidne prevlake su oksidovale na 1100 ºC pod atmosferskim pritiskom. Kinetika oksidacije aluminidnih prevlaka sa rodijumom i platinom je bila slična, ali se razlikovala od kinetike oksidacije obične prevlake. Glavni proizvod u rodijumom i platinom modifikovanim prevlakama bio je α-Al_2O_3 nakon 360 h oksidacije. Pored β-NiAl je identifikovana i γ-Ni_3Al faza. Prisustvo 4 at. % rodijuma u prevlaci je omogućilo sličnu otpornost na oksidaciju kao prisustvo 10-20 at. % platine. I rodijum i platina inkorporirani u aluminidnoj prevlaci proizvedeni postupkom hemijske depozicije pare su pružili zaštitu od oksidacije superleguri Inconel 713.

Ključne reči: *Superlegura; Platina; Rodijum; Oksidacija; Aluminidi*